Contribution from the School of Chemical Sciences,
University of Illinois, Urbana, Illinois 61801

Nuclear Quadrupole Coupling in Octahedral Copper(II). EPR of Copper-Doped $MgSO_4 \cdot 7D_2O$: A Test of Predictions

EDWARD P. DULIBA, GREGORY C. HURST, and R. LINN BELFORD*

Received December 17, 1980

Predictions of the nuclear quadrupole coupling constants for octahedral copper(II) and the applicability of computer simulation methods to extract quadrupole coupling data from EPR of powders are confirmed with ^{63}Cu and ^{65}Cu doped into $MgSO_4 \cdot 7D_2O$ as a test case. From orientation-dependent EPR spectra of each isotope, both as oriented single crystals and as powders, the following spin-Hamiltonian is deduced for ^{63}Cu: $\mathcal{H} = \beta \mathbf{B} \cdot \mathbf{g} \cdot \mathbf{S} + h\mathbf{I} \cdot \mathbf{A} \cdot \mathbf{S} - g_n \beta_n \mathbf{B} \cdot \mathbf{I} + h(\mathrm{QD})(I_z^2 - {}^5/_4) + h(\mathrm{QE})(I_x^2 - I_y^2)$, where $g_x = 2.0977$, $g_y = 2.0898$, $g_z = 2.4386$, $A_x = -48.9$ MHz, $A_y = -45.0$ MHz, $A_z = -362.0$ MHz, QD = 29 MHz, QE = 5 MHz, and the principal axis systems for **Q** and **A** coincide and are not far from that of **g**. The QD value is among the largest known for Cu(II), a proposed characteristic of the octahedral CuO_6 grouping. For some magnetic field orientations, secondary ($|\Delta m_I| = 1$) and tertiary ($|\Delta m_I| = 2$) transitions are important and the primary ($\Delta m_I = 0$) transitions are strongly affected by quadrupolar effects. The powder and single-crystal methods yield parameters in good agreement.

Introduction

The determination of nuclear quadrupole coupling information from single-crystal EPR data for copper(II) paramagnetic centers was proposed by Bleaney et al.,[1-3] and the efficacy of the method has been well established by several studies.[1-13] Nuclear quadrupole coupling can affect the EPR spectrum by enhancing normally forbidden transitions ($\Delta m_I \neq 0$, nonprimary) and altering the line positions of all transitions. In this laboratory, we have found good correlations between the principal nuclear quadrupole coupling constant and the site symmetry for copper(II) paramagnetic centers in oxygen coordination environments.[4,5,9,10,12,14] The largest values have corresponded to the most symmetric systems, octahedral ones, but rather few cases have been studied. Recent studies of copper-doped $MgSO_4 \cdot 7H_2O$ single crystals omitted the effects of nuclear quadrupole interaction,[15a] whereas an old report[15b] noted these effects but provided no quantitative analysis. Our previous work on oxygen-coordinated Cu(II) in various symmetries would lead us to predict, for this fairly ionic, octahedrally symmetric environment, a large principal nuclear quadrupole coupling constant of QD $\sim$ 30–33 MHz with a substantial effect on the EPR spectrum. To test this prediction, we have investigated the EPR spectra of ^{63}Cu- and ^{65}Cu(II)-doped $MgSO_4 \cdot 7D_2O$ at both X- and Q-band frequencies.

This case provided a nice opportunity to test the reliability of our computer simulation approach[7,14,16] to the extraction of nuclear quadrupole coupling parameters from EPR spectra of powders, since we were able to study first powders[17] and then oriented single crystals. An exploratory powder analysis thus was unbiased by knowledge of single-crystal results but was then subjected to a rigorous test.

Experimental Section

Samples of ^{63}CuO and ^{65}CuO obtained from Oak Ridge National Laboratory were dissolved in a minimum quantity of concentrated sulfuric acid and mixed with a copious quantity of acetone. The resulting blue precipitate ($CuSO_4 \cdot 5H_2O$) was filtered and dehydrated by heating under vacuum to give $^{63}CuSO_4$ and $^{65}CuSO_4$. Isotopically pure copper served to avoid the complexity of spectra that would otherwise occur due to overlap of the spectra of the two naturally occurring copper nuclei. $MgSO_4$ was prepared from $MgSO_4 \cdot 7H_2O$ by heating under vacuum. From 3 mol % $CuSO_4$ added to a saturated solution of $MgSO_4$ in D_2O, good single crystals of ^{63}Cu- and ^{65}Cu-doped $MgSO_4 \cdot 7D_2O$ of orthorhombic symmetry grew by slow evaporation (3–6 days) at room temperature. We chose deuterium oxide in preference to normal water in order to maintain the EPR line widths as narrow as possible. Doped crystals contained between 0.10 and 0.50 mol % copper. Crystals with well-developed faces were used and identified by comparison with the crystal morphology described by Viola.[18] Knowing the morphology, we used an optical goniometer to align crystal planes and then transferred the crystals to quartz rods.

EPR single-crystal spectra were recorded at X-band frequencies (9.5 GHz) on a Varian E-9 spectrometer and at Q-band frequencies (35 GHz) on a Varian E-16 spectrometer. X-band frequencies were determined with a Hewlett-Packard 5240-A digital frequency meter. A speck of DPPH ($g = 2.0036$) was used to determine frequencies for the Q-band spectra. Magnetic fields were calibrated with a Bruker B-NM20 tracking NMR oscillator. The temperature was maintained at 180 K by a Varian V-4540 variable-temperature accessory utilizing a cooled nitrogen gas stream. Single-crystal spectra were recorded every 10° through 200° in three perpendicular planes. Powder spectra were also recorded at X- and Q-band frequencies. In the preliminary powder study of a ^{63}Cu specimen, fields and frequencies were not calibrated accurately; the subsequent powder study of both ^{63}Cu and ^{65}Cu specimens incorporated the same precise calibrations as were employed for the single-crystal work.

Computer simulations of the single-crystal and powder spectra used programs developed by Nilges and Belford and described elsewhere.[7] Line positions are determined by diagonalization of the spin-Hamiltonian matrix. For powder simulations, a four-point Gauss-point integration is used. The programs allow consideration of **g**, hyperfine, isotropic nuclear **g**, nuclear quadrupole, and superhyperfine matrices and nonalignment of the principal axes of the **g**, hyperfine, superhyperfine, and quadrupole matrices. Calculations utilized the University of Illinois IBM 360 computer and VAX-11 computer, and simulations were plotted on Houston Instruments digital plotters.

Results

Our initial study[17] was of the powder near 120 K. Successful simulations of the spectra (by program QPOW[7]) required

(1) Bleaney, B. *Philos. Mag.* **1951**, *42*, 441.
(2) Bleaney, B.; Bowers, K. D.; Ingram, D. J. E. *Proc. R. Soc. London, Ser. A.* **1955**, *228*, 147.
(3) Bleaney, B.; Bowers, K. D.; Pryce, M. H. L. *Proc. R. Soc. London, Ser. A* **1955**, *228*, 166.
(4) So, H.; Belford, R. L. *J. Am. Chem. Soc.* **1969**, *91*, 2392.
(5) So, H. Ph.D. Thesis, University of Illinois, Urbana, IL, 1970.
(6) White, L. K.; Belford, R. L. *J. Am. Chem. Soc.* **1976**, *98*, 4428.
(7) Nilges, M. J. Ph.D. Thesis, University of Illinois, Urbana, IL, 1979. Belford, R. L.; Nilges, M. J. Paper No. 59, Symposium on Electron Paramagnetic Resonance Spectroscopy, Rocky Mountain Conference on Analytical Chemistry, Denver, Aug 1979, to be published.
(8) So, H.; Belford, R. L. *Phys. Rev. B: Solid State* **1970**, 3810.
(9) Belford, R. L. Inorg. Paper No. 86, Symposium on Structural Information from Electric Field Gradient Measurements, American Chemical Society, Philadelphia, April 1975.
(10) Belford, R. L. International ESR Symposium, Royal Dutch Chemical Society and the Chemical Society, Nijmegen, Holland, Aug 1976; also International ESR Conference of the Chemical Society, Cardiff, Wales, April 1978.
(11) deWit, M.; Reinberg, A. R. *Phys. Rev.* **1967**, *163*, 261.
(12) White, L. K.; Belford, R. L. *Chem. Phys. Lett.* **1976**, *37*, 553.
(13) Chacko, V. P.; Monoharan, P. T. *J. Magn. Reson.* **1976**, *22*, 7.
(14) Belford, R. L.; Duan, D. C. *J. Magn. Reson.* **1978**, *29*, 293.
(15) (a) Radhakrishna, S.; Bhaskar Rao, T. *J. Magn. Reson.* **1978**, *32*, 71. (b) Raoult, G.; Duclaux, A.-M. *Arch. Sci.* **1960**, *13*, 199.
(16) Northern, T. M. Ph.D. Thesis, University of Illinois, Urbana, IL, 1976.
(17) Hurst, G. C. B.S. Thesis, University of Illinois, Urbana, IL, 1979.
(18) Viola, C. *Z. Kristallogr.* **1923**, *58*, 583.

0020-1669/82/1321-0577$01.25/0

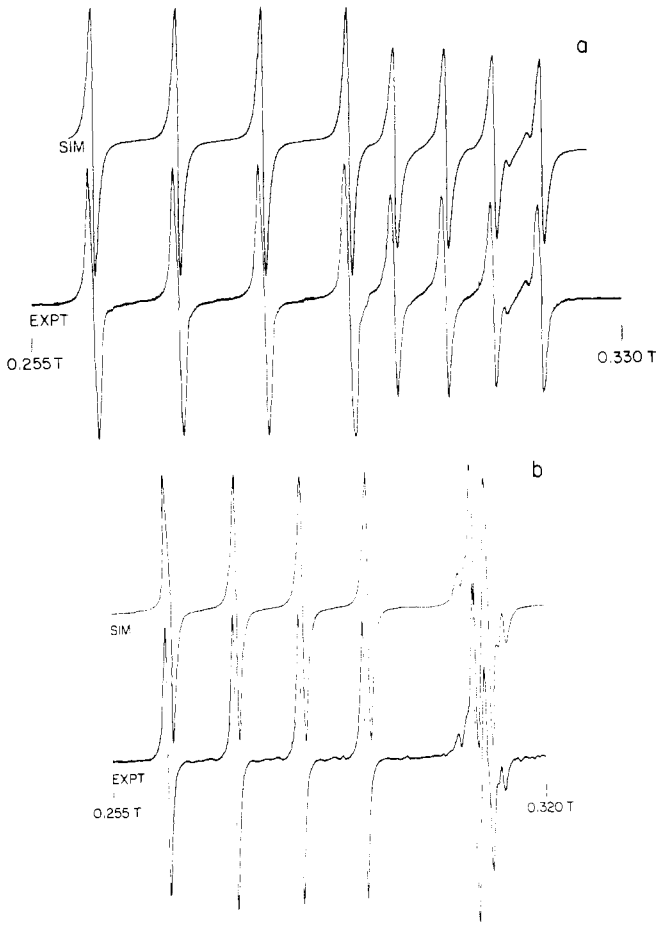

Figure 1. Example of the fit between the experimental and simulated EPR spectra of a $^{65}Cu:MgSO_4 \cdot 7D_2O$ single crystal in the *bc* plane. Instrument parameters: ν = 9.1062 GHz, 100-mT scan range centered at 290 mT, time constant = 0.03 s, 0.008-mT peak-to-peak modulation at 100 kHz, microwave power = 2.0 mW, receiver gain = 800, temperature = 180 K. Simulation parameters: ν = 9.1062 GHz, g_x = 2.0977, g_y = 2.0898, g_z = 2.4386, A_x = −51.6 MHz, A_y = −48.3 MHz, A_z = −379.5 MHz, QD = 27 MHz, QE = 4 MHz, Lorentzian line widths of 26, 26, and 36 MHz for the *x*, *y*, and *z* components, respectively, and g_n = 1.587.[22] (a) 31.5° from the *c* axis. (b) 58.5° from the *c* axis. Note the distortion in one of the quartets due to the large nuclear quadrupole interaction at this angle.

substantial rhombic terms and a larger quadrupole coupling constant—QD ≈ 32 MHz. The subsequent, more detailed, work on single crystals and powders was carried out at 180 K and with much greater attention to accurate measurements of fields and frequencies. The agreement with the initial powder result was satisfactory and confirmed that we can determine nuclear quadrupole coupling constants quite well by simulations of powder spectra.

Single-crystal spectra for which the magnetic field does not lie in a primary—(100), (010), or (001)—crystallographic plane show the 16 lines of four sets of primary ($\Delta m_I = 0$) hyperfine quartets due to $I = {}^3/_2$ for both ^{63}Cu and ^{65}Cu, consistent with the magnesium host crystal's $P2_12_12_1$ space group with four magnetic sites . The X-ray determination of crystal structure has been reported by Baur.[19] Each metal cation is octahedrally coordinated by six oxygen atoms of the water molecules, with the seventh water molecule occupying an interstitial site. The single-crystal spectra for which the magnetic field lies in general positions in primary crystallographic planes show eight lines, as in Figure 1a. In many orientations, the large nuclear quadrupole interaction causes

(19) Baur, W. H. *Acta Crystallogr.* **1964**, *17*, 1361.

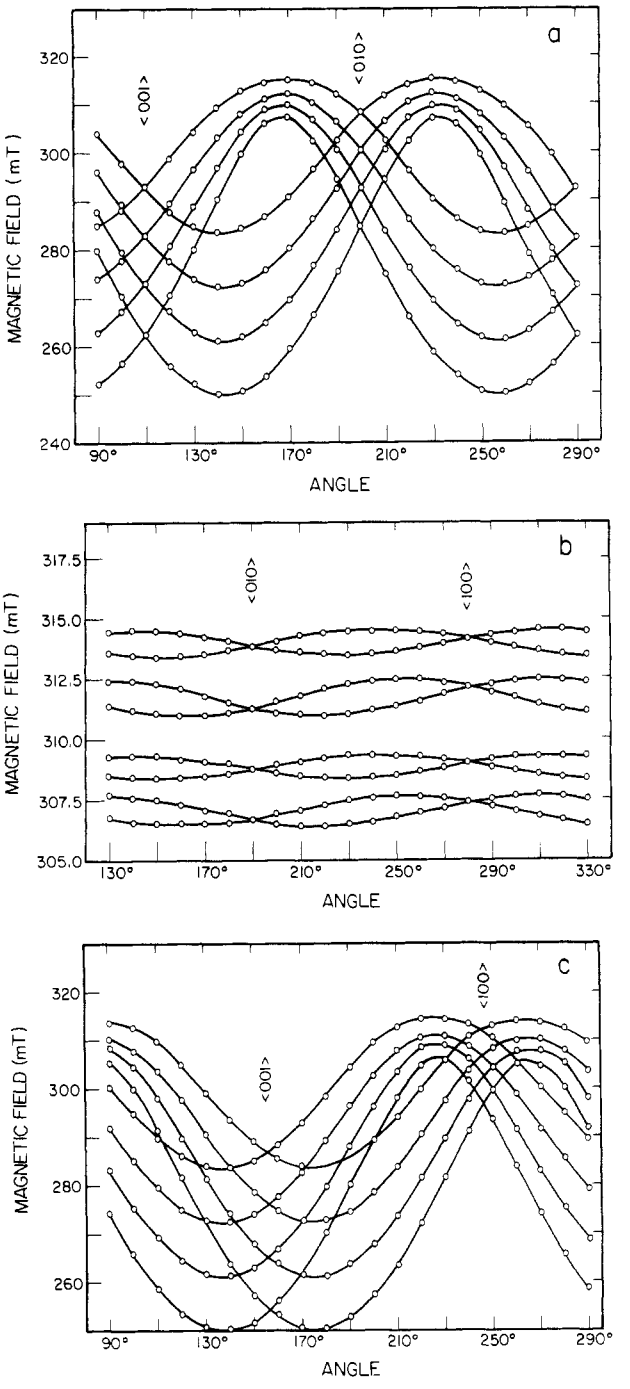

Figure 2. Angular variation of the EPR spectrum of $^{65}Cu:MgSO_4 \cdot 7D_2O$ at 180 K. The curves are least-squares fits of eq 2 and 3 for (a) the *ab* plane, (b) the *bc* plane, and (c) the *ac* plane.

distortion of the quartets normally present; for example, see Figure 1b. The two quartets become equivalent when the magnetic field is parallel to one of the primary crystallographic axes. Angular variation of the spectra is shown for the three perpendicular planes in Figure 2 for the ^{65}Cu-doped single crystal. Examination shows that the principal axes of the **g** matrix closely correspond to the crystallographic axes. The spectra were fitted to the spin-Hamiltonian of eq 1, including

$$\mathcal{H} = \beta(g_xB_xS_x + g_yB_yS_y + g_zB_zS_z) + h(S_zA_zI_z + S_xA_xI_x + S_yA_yI_y) - \beta_n g_n(B_xI_x + B_yI_y + B_zI_z) + h(\mathrm{QD})[I_z^2 - I(I+1)/3] + h(\mathrm{QE})(I_x^2 - I_y^2) \quad (1)$$

nuclear quadrupole and isotropic nuclear Zeeman terms, where the (*x*, *y*, *z*) axis systems may be different for the **g**, **A**, and **Q** matrices.

Table I. Principal Values of the g, Hyperfine, and Quadrupole Matrices from Single-Crystal Data[a]

nucleus	g_x	g_y	g_z	A_x, MHz	A_y, MHz	A_z, MHz	*a*, deg	*b*, deg	*c*, deg	QD, MHz	QE, MHz
^{63}Cu	2.0977	2.0898	2.4386	−48.9	−45.9	−362.0	63	1	132	29	5
^{65}Cu	2.0977	2.0898	2.4386	−51.6	−48.3	−379.5	55	2	129	27	4

[a] Estimated errors: for the *g* values +0.0015, for the hyperfine values ±1.0 MHz, for the quadrupole values ±1.5 MHz, and for the Euler angles of the hyperfine matrix ±3°.

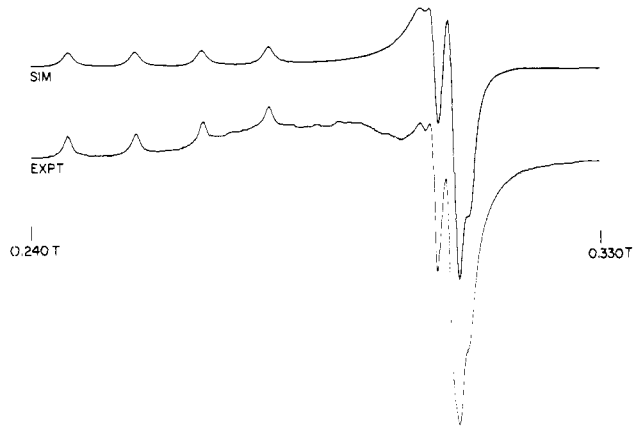

Figure 3. Best fit between the experimental and simulated EPR spectra of ^{65}Cu:$MgSO_4 \cdot 7D_2O$ powder. Instrument parameters: ν = 9.1049 GHz, 90-mT scan range centered at 285 mT, time constant = 0.30 s, 16-min scan, 0.04-mT peak-to-peak modulation at 100 kHz, microwave power = 1.5 mW, receiver gain = 800, temperature = 180 K. Simulation parameters: ν = 9.1049 GHz, g_x = 2.0977, g_y = 2.0898, g_z = 2.4386, A_x = −51.6 MHz, A_y = −48.3 MHz, A_x = −379.5 MHz, QD = 27 MHz, QE = 4 MHz, Lorentzian line widths of 24, 24, and 33 MHz for the *x*, *y*, and *z* components, respectively, and g_n = 1.587.[22]

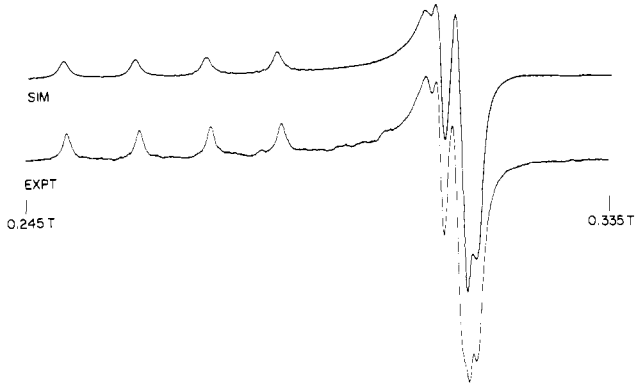

Figure 4. Best fit between the experimental and simulated EPR spectra of ^{63}Cu:$MgSO_4 \cdot 7D_2O$ powder. Instrument parameters: ν = 9.1090 GHz, 90-mT scan range centered at 285 mT, time constant = 0.03 s, 16-min scan, 0.04 mT peak-to-peak modulation at 100 kHz, microwave power = 2.5 mW, receiver gain = 250, temperature = 180 K. Simulation parameters: ν = 9.1090 GHz, g_x = 2.0977, g_y = 2.0898, g_z = 2.4386, A_x = −48.9 MHz, A_y = −45.9 MHz, A_z = −362.0 MHz, QD = 29 MHz, QE = 5 MHz, Lorentzian line widths of 31, 31, and 37 MHz for the *x*, *y*, and *z* components, respectively, and g_n = 1.482.[22]

Field positions from each plane were fitted via least-squares analysis to eq 2 and 3. The resulting $\mathbf{g}^2$ and $\mathbf{g}^2\mathbf{A}^2$ matrices

$$\mathbf{g}^2 = g_{ii}^2 \sin^2\theta + 2g_{ij}^2 \sin\theta\cos\theta + g_{jj}^2\cos^2\theta \quad (2)$$

$$\mathbf{g}^2\mathbf{A}^2 = g_{ii}^2A_{ii}^2 \sin^2\theta + 2g_{ij}^2A_{ij}^2 \sin\theta\cos\theta + g_{jj}^2A_{jj}^2\cos^2\theta \quad (3)$$

were diagonalized to give the principal *g* and *A* values (see Table I). For ^{65}Cu, the Euler angles of the hyperfine matrix with respect to the principal axis system for the **g** matrix were a = 55°, b = 2°, and c = 129°, in the convention of Rose.[20]

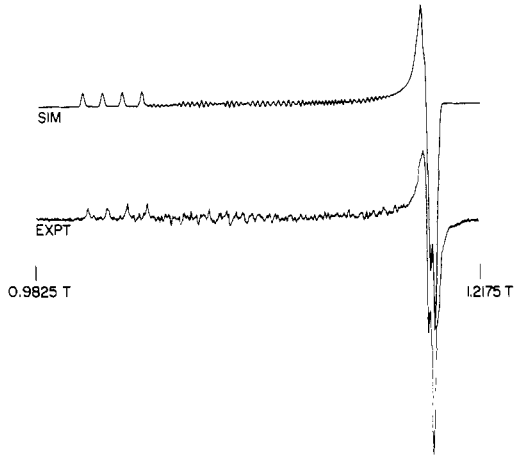

Figure 5. Fit between the experimental and simulated EPR spectrum of ^{63}Cu:$MgSO_4 \cdot 7D_2O$ powder. Instrument parameters: ν = 34.88 GHz, 235-mT scan range centered at 1.010 T, time constant = 0.1 s, 4-min scan, 0.025-mT peak-to-peak modulation at 100 kHz, microwave power = 0.5 mW, receiver gain = 250, temperature = ~77 K. Simulation parameters: ν = 34.88 GHz, g_x = 2.0977, g_y = 2.0898, g_z = 2.4386, A_x = −48.9 MHz, A_y = −45.9 MHz, A_z = −362.0 MHz, QD = 29 MHz, QE = 5 MHz, Gaussian line widths of 29, 29, and 32 MHz for the *x*, *y*, and *z* components, respectively, and g_n = 1.482.[22]

Table II. Reports of the g and Hyperfine Matrix Values at Different Temperatures

temp, K	g_x	g_y	g_z	A_x, MHz	A_y, MHz	A_z, MHz
120[a]	2.0995	2.0897	2.4480	−55	−54	−362
150[b]	2.098	2.089	2.441	−66	−54	−348
180[c]	2.0977	2.0898	2.4386	−48.9	−45.9	−362.0
300[b]	2.127	2.127	2.398			−216

[a] This study; cf. ref 17; uncertainties in *g* values ±0.002, in hyperfine values ±1 MHz. Values are based on a computer simulation of X-band powder spectrum. [b] Reference 15; uncertainties in *g* values ±0.002 at 150 K, in hyperfine values ±3 MHz at 150 K, in *g* values ±0.005 at 300 K. [c] This study.

For ^{63}Cu, the Euler angles were a = 58°, b = 1°, and c = 125°. Best-visual-fit computer simulations of the single-crystal spectra were used to confirm and refine these values and determine the quadrupole matrix. For ^{65}Cu, the Euler angles of the principal axes of the **g** matrix of the four sites in each unit cell with respect to the crystallographic axes were found: site 1, a = 89°, b = 35°, c = 61°; site 2, a = 26°, b = −35°, c = 61°; site 3, a = 89°, b = −35°, c = 61°; site 4, a = −26°, b = −35°, c = −60°. For ^{63}Cu, the Euler angles of the principal axes of the **g** matrix of the four sites were as follows: site 1, a = 88°, b = 35°, c = 61°; site 2, a = −27°, b = −35°, c = 60°; site 3, a = 88°, b = −35°, c = −61°; site 4, a = −27°, b = −35°, c = −60°. Notice that the small differences in Euler angles between the two isotopes must reflect measurement error.

Subsequently, new powder spectra of ^{63}Cu- and ^{65}Cu-doped $MgSO_4 \cdot 7D_2O$ were obtained both to check the values found

(20) Rose, M. E. "Elementary Theory of Angular Momentum"; Wiley: New York, 1957.
(21) Sternheimer, R. M. *Phys. Rev.* **1967**, *154*, 10.

Table III. Site Symmetry Dependence of Nuclear Quadrupole Coupling Values for ^{63}Cu(II) Coordinated by Oxygen Atoms

site symmetry	QD, MHz	QE, MHz	system
octahedron	30.0–33.0		copper-doped Tutton salts,[a] $Zn(HCO_2)\cdot 2H_2O$,[4,5] TiO_2,[8] and BeO[11]
elongated octahedron or tetragonal pyramid	29.0 ± 1.5	5.0 ± 1.5	$Cu:MgSO_4\cdot 7D_2O$, 180 K (this study)
	~32 ± 2		same, 120 K, powder, QE not included
	25.5–19.8		solutions of $Cu((CH_3CO)CH)_2$ in C_6H_5N, C_2H_5OH, and $CHCl_3$[14]
	18.0		$Cu:Zn(C_{10}O_2H_9)_2\cdot C_2H_5OH$[5]
intermediate (flattened) tetrahedron or square with some out-of-plane coordination	15.9, 18.6		$Cu:Zn((CH_3)_3CCO)_2CH_2$, $CaCd(CH_3CO_2)_4\cdot 6H_2O$[4,5,9,10]
square plane	13.5		$Cu:K_2Pd(C_2O_4)_2$[12]
	9.6–10.5		Cu bis(β-ketoenolates)[b]

[a] $K_2Zn(SO_4)_2\cdot 6H_2O$, $K_2Zn(SO_4)_2\cdot 6D_2O$, $Rb_2Zn(SO_4)_2\cdot 6H_2O$, $Rb_2Zn(SO_4)_2\cdot 6D_2O$, $(NH_4)_2Zn(SO_4)_2\cdot 6H_2O$,[1-3] and $Mg_3La_2(NO_3)_{12}\cdot 24D_2O$.[5] [b] $Cu:Pd(CH_3CO)_2CH)_2$, $Pd(C_{10}O_2H_9)_2$, $Pd((C_6H_5CO)_2CH)_2$, and solutions of $Cu((C_6H_5CO)_2CH)_2$ in $CHCl_3$ and $C_6H_5CH_3$.[5]

from the single-crystal data (see Figures 3–5) and to help us further study the precision and reliability of the powder method for determination of QD. For the computer simulations, we determined the principal values of the **g**, hyperfine, and quadrupole matrices using the Euler angles found from the single-crystal spectra.

Figure 6 compares simulations of X-band spectra of the ^{65}Cu powder for a range of quadrupole couplings. QD values are as follows: A, 30; B, 27; C, 24; and E, 0 MHz. The value determined from the powder simulation corresponds well with the single-crystal result. Figure 6E demonstrates an attempted simulation excluding the nuclear quadrupole effects.

Figure 6D exhibits the effect of the signs of the hyperfine components. On account of the interplay between the essentially quadratic behavior of quadrupole terms and the linear behavior of nuclear Zeeman and hyperfine terms upon nuclear spin quantum number, a substantial quadrupole interaction allows one to determine relative signs of hyperfine components. Without the quadrupole or nuclear Zeeman terms in the Hamiltonian, the spectrum would be unaffected by the hyperfine components' signs. In cases where the quadrupole effect is large, the effect is rather noticeable.

It is evident that spectrum B best fits the experimental spectrum. The highest field feature is the most sensitive to the value of QD. Without quadrupole coupling, no simulation came close to the appearance of the experimental spectrum. We judged that the powder simulations deviated detectably from the experimental spectrum for QD values outside the range 27 ± 1.5 MHz for ^{65}Cu or 29 ± 1.5 MHz for ^{63}Cu.

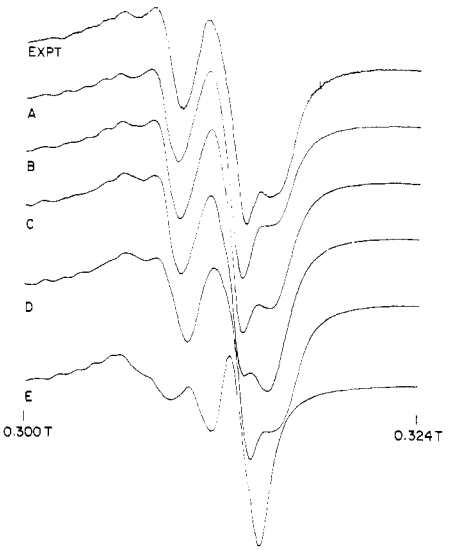

Figure 6. Experimental and simulated high-field (perpendicular) region EPR spectra of $^{65}Cu:MgSO_4\cdot 7D_2O$ powder. Instrument parameters: ν = 9.1054 GHz, 40-mT scan range centered at 310 mT, time constant = 0.3 s, 16-min scan, 0.04-mT peak-to-peak modulation at 100 kHz, microwave power = 2.0 mW, receiver gain = 800, temperature = 180 K. Simulation parameters for all simulations: ν = 9.1054 GHz, g_x = 2.0977, g_y = 2.0898, g_z = 2.4386, A_x = −51.6 MHz, A_y = −48.3 MHz, A_z = −379.5 MHz, Lorentzian line widths of 24, 24, and 33 MHz for the x, y, and z components, respectively, g_n = 1.587.[22] (A) QD = 30 MHz, QE = 4 MHz; (B) QD = 27 MHz, QE = 4 MHz; (C) QD = 24 MHz, QE = 4 MHz; (D) A_x = −51.6 MHz, A_y = 48.3 MHz, A_z = −379.5 MHz, QD = 27 MHz, QE = 4 MHz; (E) QD = QE = 0.

Discussion

As expected, and as we claimed will be true for nearly all Cu(II) ions in nearly regular octahedral sites, secondary ($|\Delta m_I| = 1$) and tertiary ($|\Delta m_I| = 2$) transitions are not negligible unless the magnetic field is aligned close to the z axis of the complex, particularly at high frequencies (e.g., Q band), where the nuclear Zeeman term is enhanced. Quadrupolar interactions substantially affect positions and intensities of the primary lines and should not be neglected in their analysis.

The hyperfine and quadrupole matrices are collinear within the experimental accuracy of this investigation. This is to be expected, as both hyperfine and quadrupole matrices are essentially properties of the ground electronic state of the system and will reflect its symmetry. Reasonable variations for all Euler angles for the quadrupole matrix were tried, but the computer simulations were not very sensitive to small amounts of matrix noncollinearity. We chose to analyze the ^{63}Cu and ^{65}Cu data independently. The ^{63}Cu:^{65}Cu ratio of hyperfine matrix elements ranges from 0.948 (x) to 0.954 (z). From the nuclear moments,[22] one expects a ratio of 0.933. This corresponds to an error of 0.8 MHz in the x component and would result from a difference of only 0.03 mT. The ^{63}Cu:^{65}Cu ratio of the quadrupole matrix elements is 1.074 (QD) and 1.25 (QE) compared to the expected ratio 1.082, again well within reasonable experimental error.

This system is temperature sensitive, as is implied by values found at several temperatures by different workers (Table II). The trend indicates a reduction in x–y anisotropy as the temperature increases. The X-ray crystal structure of $MgSO_4\cdot 7H_2O$[19] at room temperature shows three pairs of nearly equal Mg–O bond lengths: 2.045, 2.046 Å; 2.054, 2.055 Å; 2.092, 2.099 Å. The distortion of the octahedron of coordinating water molecules would appear to increase at lower temperatures according to the **g** matrix data. A small change in the interatomic distances could account for the **g** matrix temperature variation.

Since the quadrupole moment is −0.195 b for ^{65}Cu and −0.211 b for ^{63}Cu,[21] the electric field gradient at the nucleus can be calculated. In the coordinate system where the quadrupole matrix is diagonal, $Q_k = -3eQeq_k/4I(2I-1)$ or $Q_k = -eQeq_k/4$ for $k = x$, y, or z. Since the matrix is traceless, QD = $Q_z - (Q_x + Q_y)/2$ and QE = $(Q_x - Q_y)/2$. For ^{65}Cu, one can use the QD and QE values from the data analysis to

(22) Fuller, G. H.; Cohen, V. W. *Nucl. Data, Sect. A* **1969**, *5*, 446.

find $Q_x = -7.6 \times 10^{-10}$ hartree, $Q_y = -2.0 \times 10^{-9}$ hartree, and $Q_z = 2.7 \times 10^{-9}$ hartree. Then $eq_x = -0.44$ au, $eq_y = -1.1$ au, and $eq_z = 1.6$ au. For ^{63}Cu, $Q_x = -7.1 \times 10^{-10}$ hartree, $Q_y = -2.2 \times 10^{-9}$ hartree, $Q_z = 2.9 \times 10^{-9}$ hartree, $eq_x = -0.38$ au, $eq_y = -1.2$ au, and $eq_z = 1.6$ au.

This compound has nuclear quadrupole coupling constants consistent with the few other $^{63}Cu(II)$ oxygen-coordinated compounds of this high symmetry, mostly octahedral, that have been examined (ref 1-5, 8-10, and 14 and Table III). This system is a slightly elongated octahedron. Its QD value is at the low end of the range of values previously found for octahedral environments but above values found for more elongated octahedra.[14] The inclusion of the QE parameter here could account for the observed reduction in the QD value. The large QD (or eq_z) value indicates an elongated distribution of charge, mainly attributable to the d_{xy} orbital vacancy in the Cu(II) valence shell, with some reduction—perhaps 25%—owing to covalent charge spreading.[4-6,10,12,23] Quantitative discussions of the relationship between QD, QE, and electronic structure are given elsewhere (e.g., ref 5, 9, 10, and 23, and work to be published). The QE value indicates some distortion from a completely axial charge distribution. The moderate rhombic component of that distribution ($eq_x - eq_y = 0.8$ au) must be related to a slight difference between two pairs of equatorial metal-oxygen bond distances revealed by the structural report on the host crystal.[19]

Finally, the utility of EPR powder spectra to determine nuclear quadrupole coupling constants has been confirmed in this study. Our predictions as well as the values initially derived from computer simulations of powder spectra were borne out by the subsequent detailed single-crystal analyses. The close agreement between the sets of EPR parameters obtained by the two methods demonstrates the adequacy of powder-spectrum simulation for the determination of nuclear quadrupole coupling constants.

Acknowledgment. This research was supported by the National Science Foundation, Quantum Chemistry Program.

Registry No. $MgSO_4 \cdot 7H_2O$, 25102-34-5; ^{63}Cu, 14191-84-5; ^{65}Cu, 14119-06-3.

(23) White, L. K. Ph.D. Thesis, University of Illinois, Urbana, IL, 1975.

Contribution from the Department of Chemistry, University of Iowa, Iowa City, Iowa 52242

Multinuclear Magnetic Resonance Spectroscopy of Spin-Admixed $S = {}^5/_2, {}^3/_2$ Iron(III) Porphyrins

ARDEN D. BOERSMA and HAROLD M. GOFF*

Received March 16, 1981

A variety of synthetic iron(III) porphyrin complexes ($Fe^{III}PorX$, X = $SO_3CF_3^-$, ClO_4^-, and $C(CN)_3^-$) were examined with multinuclear NMR spectroscopy (^1H, ^{13}C, ^{19}F, and ^{35}Cl). Deviations from NMR Curie law behavior, diminished magnetic moments, and characteristic ESR $g = 4$ values support previous evidence for the quantum-mechanical admixture of $S = {}^5/_2$ and $S = {}^3/_2$ states. NMR studies of titrations with the corresponding tetrabutylammonium salts and dipolar shift calculations show the ligands are coordinated rather than ion paired in solution. Solvent studies indicate more $S = {}^5/_2$ character is present in aromatic solvents than in chlorinated solvents. Although the tricyanomethanide complex is thought to exhibit a "pure" $S = {}^3/_2$ state in crystalline form, solution measurements are consistent with spin admixture.

Introduction

Fundamental inorganic chemical studies have demonstrated that metalloporphyrins may exhibit fascinating and often unique structural, electronic, and reactivity properties. This is illustrated, for example, in the possible spin states of iron(III) porphyrins. The high-spin state is associated with coordination of a single weak-field anionic ligand or bisligation of two weak-field ligands.[1-3] Recently an unusual spin-admixed state of $S = {}^5/_2$ and $S = {}^3/_2$ character has been postulated for certain very weak-field anionic complexes.[4-11] This state is thought to be mixed quantum-mechanically and not via thermal equilibrium. Thus, spin-orbit coupling provides a mechanism for mixing closely spaced "pure" $S = {}^5/_2$ and ${}^3/_2$ states.

Several porphyrin complexes have been prepared which are thought to show quantum-mechanical spin admixture.[4-11] The structures have been solved for iron(III) tetraphenylporphyrin perchlorate ($Fe(TPP)ClO_4$),[8,9] iron(III) tetraphenylporphyrin tricyanomethanide ($Fe(TPP)C(CN)_3$),[10] and iron(III) octaethylporphyrin perchlorate ($Fe(OEP)ClO_4$).[6] For the tricyanomethanide species a pure $S = {}^3/_2$ configuration has been assigned in the solid state on the basis of Mössbauer quadrupole splitting and structural parameters. Solution studies reported for various perchlorate complexes indicate that spin admixture ($S = {}^5/_2, {}^3/_2$) is not restricted to the solid state.[4] This admixed spin state has been postulated for cytochrome c' on the basis of reduced magnetic moment values and unusual $g = 4$ ESR signals.[12]

Solution properties of weak-field complexes have been examined in detail by multinuclear NMR methods. Rationale for this additional work is found in attempts to unequivocally demonstrate that the anionic ligand remains bound in solution and interest in examining a species with a potentially pure $S = {}^3/_2$ state. It will be demonstrated that perchlorate, trifluoromethanesulfonate, and tricyanomethanide ligands do indeed remain coordinated to synthetic iron(III) porphyrins in nonligating solvents. Further, it is shown that the pure S

(1) Scheidt, W. R. In "The Porphyrins"; Dolphin, D., Ed.; Academic Press: New York, 1978; Vol. III, Chapter 10.
(2) La Mar, G. N.; Walker, F. A. In "The Porphyrins"; Dolphin, D., Ed.; Academic Press: New York, 1978; Vol. IV, Chapter 2.
(3) (a) Mashiko, T.; Kastner, M. E.; Spartalian, K.; Scheidt, W. R.; Reed, C. A. *J. Am. Chem. Soc.* **1978**, *100*, 6354. (b) Scheidt, W. R.; Cohen, I. A.; Kastner, M. E. *Biochemistry* **1979**, *18*, 3546.
(4) Goff, H.; Shimomura, E. *J. Am. Chem. Soc.* **1980**, *102*, 31.
(5) Kobayashi, H.; Kaizu, Y.; Eguchi, K. *Adv. Chem. Ser.* **1980**, *No. 191*, 327.
(6) Masuda, H.; Taga, T.; Osaki, K.; Sugimoto, H.; Yoshida, Z.; Ogoshi, H. *Inorg. Chem.* **1980**, *19*, 950.
(7) Ogoshi, H.; Sugimoto, H.; Yoshida, Z. *Biochim. Biophys. Acta* **1980**, *621*, 19.
(8) Reed, C. A.; Mashiko, T.; Bentley, S. P.; Kastner, M. E.; Scheidt, W. R.; Spartalian, K.; Lang, G. *J. Am. Chem. Soc.* **1979**, *101*, 2948.
(9) Kastner, M. E.; Scheidt, W. R.; Mashiko, T.; Reed, C. A. *J. Am. Chem. Soc.* **1978**, *100*, 666.
(10) Summerville, D. A.; Cohen, I. A.; Hatano, K.; Scheidt, W. R. *Inorg. Chem.* **1978**, *17*, 2906.
(11) Dolphin, D. H.; Sams, J. R.; Tsin, T. B. *Inorg. Chem.* **1977**, *16*, 711.
(12) Maltempo, M. M. *J. Chem. Phys.* **1974**, *61*, 2540.

0020-1669/82/1321-0581$01.25/0